Stereomutation Tunneling Switching Dynamics and Parity Violation in Chlorineperoxide Cl−O−O−Cl†

Martin Quack* and Martin Willeke

Physical Chemistry, ETH Zurich, CH-8093 Zurich, Switzerland

Received: October 10, 2005; In Final Form: November 28, 2005

In a search for efficient spectroscopic avenues toward experiments on molecular parity violation, we investigate the stereomutation tunneling processes in the axially chiral chlorine isotopomers of Cl_2O_2 by the quasi-adiabatic channel reaction path Hamiltonian (RPH) approach and the corresponding parity violating potentials by means of quantum chemical calculations including our recently developed Multiconfiguration linear response (MC-LR) approach to electroweak quantum chemistry. The calculated ground-state torsional tunneling splittings for all isotopomers of Cl_2O_2 are much smaller than the parity violating energy differences $\Delta_{pv}E$ between the enantiomers of these molecules and therefore parity violation is predicted to dominate the quantum dynamics of stereomutation at low energies. We also compare these with torsional ground-state tunneling splittings and parity violating energy differences of the whole series of axially chiral $HXYH^{(+)}$ isotopomers (with X, Y= $Cl^{(+)}$, O, S, Se, Te). A comparison with our previous results for the homologous molecule Cl_2S_2 shows that for Cl_2O_2 a spectroscopic high-resolution analysis should be easier and the energy region of large tunneling splittings should be more easily accessible by IR excitation. We thus propose a scheme using "tunneling switching" with vibrational excitation in order to carry out the measurement of time-dependent parity violation in superposition states of initially well-defined parity. We discuss the advantages and drawbacks of such an experiment that can be carried out entirely in the IR spectral range (for Cl_2O_2 or related molecules).

1. Introduction

It is now theoretically well established that, with the parity violating weak interaction included in the standard model of high-energy physics,[1] one predicts a small parity violating energy difference $\Delta_{pv}E$ between the ground states of the enantiomers of chiral molecules, which is equivalent to a reaction enthalpy $\Delta_{pv}H_0^{\ominus}$ for the stereomutation reaction

$$R \rightleftharpoons S \quad \Delta_{pv}H_0^{\ominus} = N_A\Delta_{pv}E \tag{1}$$

Despite its small magnitude ($\Delta_{pv}H_0^{\ominus} \approx 10^{-11}$ J mol^{-1}, depending upon the molecule considered), this could have consequences for the quantum dynamics and spectroscopy of chiral molecules as well as for the question of homochirality selected in biomolecular evolution (see reviews 2−4 with many further references). Although the question has been the subject of quantitative theoretical calculations[5−17] as well as proposals and attempts for experiments[18−32] for about three decades, no successful experiment proving effects from parity violation in chiral molecules has so far been reported. The theoretical outlook for carrying out successful experiments has changed considerably with our finding that compared to the original theoretical approaches[5−7] new theoretical calculations reported about a decade ago[10−14] lead to an increase of the predicted $\Delta_{pv}E$ by about 2 orders of magnitude for the simple benchmark systems H_2O_2 and H_2S_2 and comparable increases of 1 to 2 orders of magnitude for many other molecules. This has been reconfirmed in the meantime in several independent efforts.[15−17] These theoretical developments thus provide a basis for an increased interest in carrying out spectroscopic gas-phase experiments on molecular parity violation.

The suggested experiments fall into three categories. The first kind proposes to measure frequency differences in IR spectra of chiral molecules[18−20,25,26] ($h\nu_R - h\nu_S$ in the scheme of Figure 1 and similar for microwave, NMR, or Mössbauer spectra[22,25,27]). However, even in a successful experiment of this kind, only the determination of the *difference* of parity violating energy differences (e.g., $\Delta_{pv}E^1 - \Delta_{pv}E^\circ = h\nu_R - h\nu_S$, see Figure 1) is possible, which is an obvious limitation.

The historically second proposal concerned the observation of the time-dependent amplitude of optical activity in some very special molecules, where the stereomutation tunneling splittings are of similar magnitude as the parity violating potentials.[21] The third approach is based on the use of optical transitions to intermediate excited states of well-defined parity, which are allowed by the selection rules with respect to both enantiomers and thus $\Delta_{pv}E$ can be measured either directly as a combination difference of spectral lines in the frequency domain or as a time-dependent spectral change.[2,23] A possible realization of the third approach has been suggested using excited intermediate electronic states, and some quantitative calculations have been performed for the case of 1,3-difluoroallene with planar or quasi-planar excited electronic states (see Figure 1 in ref 33). However, one might also carry out experiments in the electronic ground state only,[4] if one uses "tunneling switching" between a vibrational lower state $|0\rangle$ satisfying

$$\Delta_{pv}E^0 \gg \Delta E_{\pm}^{\ 0} \tag{2}$$

where $\Delta E_{\pm}^{\ 0}$ would be the tunneling splitting for a symmetrical

† Part of the special issue "Jürgen Troe Festschrift".

* To whom correspondence should be addressed. ETH Zürich, Laboratorium für Physikalische Chemie, ETH-Hönggerberg, HCI, CH-8093 Zürich, Switzerland. Tel: ++41 44 632 44 21. Fax: ++41 44 632 10 21. E-mail: Martin@Quack.ch.

10.1021/jp055770h CCC: $33.50
Published on Web 02/15/2006

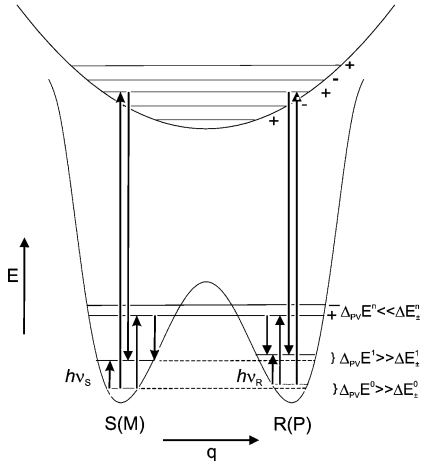

Figure 1. Scheme for the preparation of states of well-defined parity in a molecule which is chiral in the electronic ground state, with a substantial barrier for stereomutation in the ground state. In a first optical transition, one prepares a state of well-defined parity (+) in either an electronically excited state (with a low barrier or none (as shown) for stereomutation) or a highly excited torsional state (with $\Delta_{pv}E \ll \Delta E_\pm$). In a second induced transition, a state (with $\Delta E_\pm \ll \Delta_{pv}E$) with (−) parity is prepared in the ground-state potential. Also, $\Delta_{pv}E^0$ (extremely exaggerated) is indicated as the difference between the ground-state energies and $\Delta_{pv}E^1$ as the difference between the corresponding excited-state energies of the *R* and *S* enantiomers.

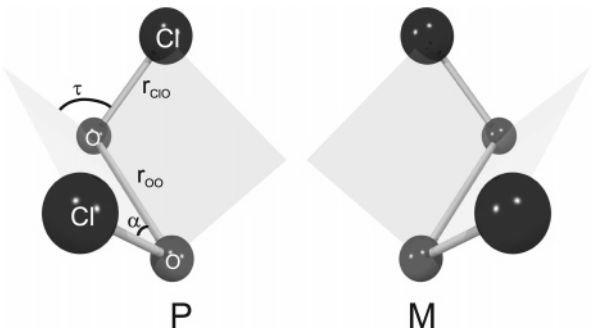

Figure 2. Chiral C_2 equilibrium structures of the *P* and *M* enantiomers of Cl_2O_2 obtained by employing MP2/aug-cc-pVTZ calculations.

(in this case hypothetical) parity conserving potential and a vibrationally excited level satisfying

$$\Delta E_\pm{}^n \gg \Delta_{pv}E^n \tag{3}$$

where therefore the wave functions have essentially well-defined parity. This scheme is outlined in Figure 1 as well. The aim of the present paper is to present theoretical proof of principle calculations on a real, spectroscopically accessible, axially chiral molecule Cl−O−O−Cl (Figure 2), which satisfies the quantitative conditions required for the use of this scheme of tunneling switching in the electronic ground state. Such an investigation on Cl_2O_2 will also complement our search for suitable simple molecular systems for such experiments, where we have especially focused on axially chiral dichalcogenides of the type X_2Y_2 (X= H, D, T, Cl and Y= O, S, Se, Te) as well as HSOH and $HOClH^+$ [10−14,34−40] among other molecules (such as isotopically chiral methanol[41,42] or $P^{35}Cl^{37}ClF$[43]). One important result of these theoretical investigations was the observation that the condition $\Delta_{pv}E \gg \Delta E_\pm$ is fulfilled for Cl_2S_2,[38] T_2Se_2,[39] D_2Te_2, and T_2Te_2,[40] and these molecules could therefore in principle be useful for an experimental study of molecular parity violation as described above. However, regarding the accessibility and spectroscopic properties, Cl_2O_2 may be superior to these molecules, as we discuss here.

Chlorine peroxide (Cl−O−O−Cl) itself has previously received attention in the quite different context of the role of the ClO dimer isomers in the catalytic cycle of ozone depletion in the springtime in the Antarctic stratosphere as well as in the Arctic. Therefore much experimental work exists on the preparation (via photolysis[44] or ClO dimerization[45,46]), the structure,[47] the rovibrational[45,48−50] and UV spectra,[44,45] the kinetics of decomposition,[51,52] the detection in the stratosphere,[53] and the ionization energy[54] (see also the Nobel prize lectures of Molina[55] and Rowland[56] and references therein) as well as theoretical work.[57−75] One main result of the theoretical investigations employing CCSD(T) calculations was that Cl−O−O−Cl may be one of the lowest energy isomers of the dimer $(ClO)_2$,[57,59] which was supported recently (e.g., refs 72 and 73) with density functional theory calculations. In a forthcoming paper, we shall address this issue at a very high level of theory.[76] The torsional barriers in Cl_2O_2 were recently examined theoretically[60,62,69] and compared with a crude experimental estimation.[47] In ref 62, the five lowest torsional energy levels are reported but not the corresponding torsional tunneling splittings. Results of high-level ab initio investigations shedding new light on the relative energies of the various isomers and transition states of chlorine dioxide will be presented elsewhere.[76] Here, we report the first investigations of parity violation in Cl−O−O−Cl. In the first part of our paper, we present the theory and computational methods for the calculations of the stereomutation tunneling splitting and the parity violating potentials in Cl−O−O−Cl. In the second part, we present our results and discuss the relation to other molecules investigated previously and furthermore the consequences for the spectroscopic detection of molecular parity violation.

2. Theory and Methods of Calculation

2.1. Electronic Structure Calculations with Parity Conservation. The calculations of the electronic energy, forces, and force constants as needed for the reaction path calculations as well as the calculation of the electric dipole moment were carried out with the Gaussian 03[77] program package. Electron correlation was included using the second-order Møller−Plesset perturbation theory (MP2) and coupled-cluster theory including single and double excitations with perturbative noniterative inclusion of triple excitations (CCSD(T)). For the choice of an appropriate basis set, we performed several calculations using progressively larger basis sets employing the 6-31+G*, 6-311+G*,[78−80] aug-cc-pVDZ, aug-cc-pVTZ, and aug-cc-pVQZ[81] standard basis sets and the MP2 level of theory. The same basis sets were also used for the CCSD(T) calculations with one exception for the aug-cc-pVQZ, which will be presented elsewhere.[76]

The values for the fundamental band strengths in terms of the corresponding integrated cross sections G_i are calculated in the double harmonic approximation and are defined through the practical eq 4[82]

$$G_i = \frac{8\pi^3}{(4\pi\epsilon_o)(3\mathrm{hc})} |\langle v_i = 1|\mu|v_i = 0\rangle|^2 \cong 41.624 \left(\frac{|\langle v_i = 1|\mu|v_i = 0\rangle|}{\mathrm{debye}}\right)^2 \mathrm{pm}^2 \tag{4}$$

where μ is the electric dipole moment operator. The electric dipole moment is linearly extrapolated along the normal coordinates. Reporting G_i has the advantage in contrast to the frequently reported $A_i = \omega_i N_A G_i$ that no additional error is

introduced in G_i through the usually large ab initio error in the harmonic wavenumbers ω_i.

2.2. Calculation of Parity Violating Potential Energies. Under field free condition and upon neglecting smaller terms arising from nuclear spin interaction, electron−electron interactions, and so forth,[11] the parity violating electroweak Hamiltonian which transforms odd under space inversion (or parity) is given by[11,13,31,83]

$$\hat{H}_{\mathrm{pv}} \approx \frac{\pi G_{\mathrm{F}}}{m_e c h \sqrt{2}} \sum_a Q_{\mathrm{W}}(a) \sum_i [\vec{s}_i \cdot \vec{p}_i \cdot \delta^3(\vec{r}_i - \vec{r}_a) + \delta^3(\vec{r}_i - \vec{r}_a) \cdot \vec{s}_i \cdot \vec{p}_i] \quad (5)$$

with the Fermi coupling constant $G_{\mathrm{F}} \approx 1.16639 \times 10^{-5} (\hbar c)^3 \times (\mathrm{GeV})^{-2} \approx 1.43586 \times 10^{-62}$ J m^3, the electron mass m_e, the velocity of light c, and Planck's constant $\hbar = (h/2\pi)$, $\vec{s}_i$ denotes the electron spin and $\vec{p}_i$ the electron momentum operator. In eq 5, the summation is carried out over nuclei a and electrons i. The weak charge $Q_{\mathrm{W}}(a)$ of nucleus a is given by

$$Q_{\mathrm{W}}(a) = Z_a(1 - 4 \cdot \sin^2 \Theta_{\mathrm{W}}) - N_a \quad (6)$$

where N_a denotes the neutron number, Z_a the proton number of nucleus a, and Θ_{W} the Weinberg angle with $\sin^2 \Theta_{\mathrm{W}} \approx 0.23117(16)$.[84]

Equation 5 was used to determine the parity violating potential energy E_{pv} as a function of the reaction path (described in detail in the next section), which was calculated as a minimum energy path with the corresponding dihedral angle τ as the leading coordinate (Figure 2), providing a set of coordinates. These have been used as input to our modified version[13] of the DALTON program package,[85] where our modified programs include the MC-LR approach based on the theory described in ref 13 to determine E_{pv}. In the present work, we used the "random phase approximation" (RPA), as described in detail elsewhere (see refs 13, 29, 86, and 87 and references cited therein).

2.3. Reaction Path Hamiltonian Calculation. Figure 2 shows the axially chiral equilibrium structures and coordinate definitions of the C_2-symmetric Cl_2O_2 enantiomers.

The torsional tunneling dynamics were calculated with the quasi-adiabatic channel reaction path Hamiltonian (RPH) approach described in detail in refs 34, 35, 39, and 37. Our treatment is a modified version of the RPH approach of Miller, Handy, and Adams[88] and is conceptually related to the adiabatic channel model.[89−92]

In this approach, the complete vibrational Hamiltonian

$$\hat{H}(\hat{p}, q, \{\hat{P}_k, Q_k\}) = \hat{H}_Q(\{\hat{P}_k, Q_k\}; q) + \hat{H}_q(\hat{p}, q) \quad (7)$$

is divided into two parts. The first part depends on the "fast" $3N - 7$ mass-weighted normal coordinates, Q_k, and their conjugate momenta, $\hat{P}_k$, and parametrically (indicated by the semicolon) upon q. The second part, which is the one-dimensional (1D) Hamiltonian $\hat{H}_q(\hat{p}, q)$, depends only on the "slow" reaction coordinate q and its conjugate momentum $\hat{p}$ and is given by

$$\hat{H}_q = \frac{1}{2} \hat{p} G \hat{p} + u(q) + V_{\mathrm{el}}(q) \quad (8)$$

with $u(q)$ as the pseudopotential (see ref 93), V_{el} as the Born−Oppenheimer potential energy along the minimum energy path, and G as the effective inverse reduced mass.

For the full Hamiltonian $\hat{H}$, the eigenfunctions are as follows

$$\Psi_m^{(n)}(\vec{Q}, q) = \chi_m^{(n)}(q) \varphi_n(\vec{Q}; q) \quad (9)$$

$$(\langle \varphi_n | \hat{H} | \varphi_n \rangle_Q - E_m^{(n)}) \chi_m^{(n)}(q) = 0 \quad (10)$$

where $\varphi_n(\vec{Q}; q)$ represents the eigenfunctions of the Hamiltonian (eq 7) at fixed values of q. We approximated these eigenfunctions by a product of 1D harmonic oscillator functions $\psi_{n_k}^{(k)}(Q_k; q)$ so that n becomes a multi-index

$$\varphi_n(\vec{Q}; q) = \prod_{k=1}^{3N-7} \psi_{n_k}^{(k)}(Q_k; q) \quad (11)$$

The potential energy along the reaction path is calculated as a minimum energy path. This reaction path is determined as follows. For a given fixed dihedral angle τ, we optimize all the remaining degrees of freedom with respect to minimum electronic potential energy (corresponding to a "clamped coordinate" approach). This "minimum energy" path has the advantage that it is invariant under isotopic substitution. The path itself was calculated in steps of 10°. A spline interpolation in the path length coordinate q employing the calculated points led to a path consisting of 179 grid points. Finally, eq 10 was solved numerically in a discrete variable representation.[34,35,94−97] We used a 128-bit word length (quadruple precision) for a floating-point number and fitted the effective potentials, all harmonic transition wavenumbers ($\omega_i(q)$), and the effective inverse reduced masses both as functions of the reaction coordinate with a Fourier series, which acted as simple filter for the numerical noise. Such a filtering scheme is necessary to achieve the desired precision. This procedure is described in more detail in refs 36 and 38 and enables us to numerically "resolve" even tunneling splittings of about 10^{-28} cm^{-1} (see ref 38). We furthermore determined for Cl_2O_2 within our RPH model the band strengths of the calculated transitions in terms of the integrated cross section $G_{t,0}$

$$G_{t,0} = \frac{8\pi^3}{(4\pi\epsilon_o)(3hc)} |\langle \Psi_t^{(\vec{0})}(\vec{Q}, q) | \mu | \Psi_0^{(\vec{0})}(\vec{Q}, q) \rangle|^2 \cong 41.624 \left(\frac{|\langle \Psi_t^{(\vec{0})}(\vec{Q}, q) | \mu | \Psi_0^{(\vec{0})}(\vec{Q}, q) \rangle|}{\mathrm{debye}} \right)^2 \mathrm{pm}^2 \quad (12)$$

If a linear extrapolation of the electric dipole moment along the normal coordinates at each point of the reaction path is appropriate, then the band strength $G_{t,0}$ can be approximated by

$$G_{t,0} \cong 41.624 \left(\frac{|\langle \chi_t^{(\vec{0})}(q) | \mu(q) | \chi_0^{(\vec{0})}(q) \rangle|}{\mathrm{debye}} \right)^2 \mathrm{pm}^2 \quad (13)$$

Equation 13 can be deduced from eq 12 with the approximation eq 11 and employing

$$\langle \varphi_0(\vec{Q}; q) | \mu(q, \vec{Q}) | \varphi_0(\vec{Q}; q) \rangle_q = \mu(q, \vec{Q} = 0) \equiv \mu(q) \quad (14)$$

This approximation has been used for the present calculations. Similar calculations can be carried out for hot band torsional transitions replacing $\Psi_0^{(\vec{0})}$ by $\Psi_k^{(\vec{0})}$ in eq 12, $\chi_0^{(\vec{0})}$ by $\chi_k^{(\vec{0})}$ (eq 13) and φ_0 by φ_k (eq 14) giving $G_{t,k}$.

The accuracy of our quasi-adiabatic channel reaction path Hamiltonian was tested for H_2O_2 by comparison with numerically exact (discrete variable) calculations[35] on a full 6D

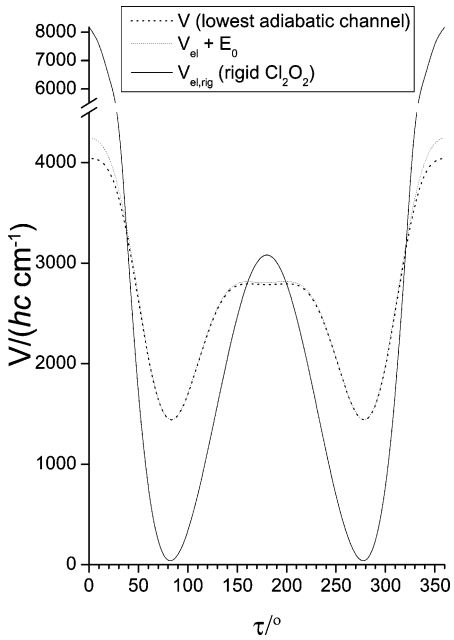

Figure 3. Various parity conserving torsional potentials plotted as a function of the dihedral angle τ: bare electronic potential for rigid Cl_2O_2 (full line), the lowest adiabatic reaction channel (dashed line), and the bare electronic potential (with structures for Cl_2O_2 from energy minimization) shifted by the equilibrium energy ($E_0 \equiv E'_z(\tau_e)$) of the lowest adiabatic channel (dotted line), that is, the zero point energy at τ_e for all coordinates except the zero point energy of the reaction coordinate.

potential hypersurface.[98] One can expect fairly accurate results using the RPH approximations except in cases of resonance interactions with close lying excited levels of nontorsional modes.

3. Results and Discussion

3.1. Reaction Path, Stationary Points, and Lowest Adiabatic Channel. Figure 3 shows a survey of the bare electronic potential (shifted by the zero point energy $E_0 = E'_z(\tau_e)$, without torsion, at the equilibrium torsional angle τ_e) and the lowest quasi-adiabatic channel potential as a function of the dihedral angle τ calculated with MP2/aug-cc-pVTZ along the reaction path.

Only small differences are visible between these two potentials except for $\tau \approx 0°$ and 360°. This implies that the zero point energy changes only in a minor way along the reaction path. The top of the barrier near the optimized $\tau = 180°$ trans structure is fairly flat over a broad range from around 130° to 230° instead of a perhaps expected sinusoidal function. This result is almost independent of the precise details of the ab initio calculation. Figure 3 shows also the electronic potential for a rigid Cl_2O_2 model ("rigid" means here without any geometry optimization along the reaction path and employing the equilibrium values of all nontorsional structure parameters) as function of τ. In this case, a sinusoidal function is obtained but the barrier heights are more than two times higher than those for the potential where the structure is optimized at each value of τ. This implies that in the region of the $\tau = 180°$ trans structure the electronic potential energy increase is flattened through a rearrangement of the remaining structure parameters. In Figure 4, the optimized structure parameters r_{OO} and r_{ClO} and the angle α_{ClOO} are shown as function of τ. The angle α exhibits a large dependence on τ and decreases by about 10° when going from the cis to the trans structure. A relatively large

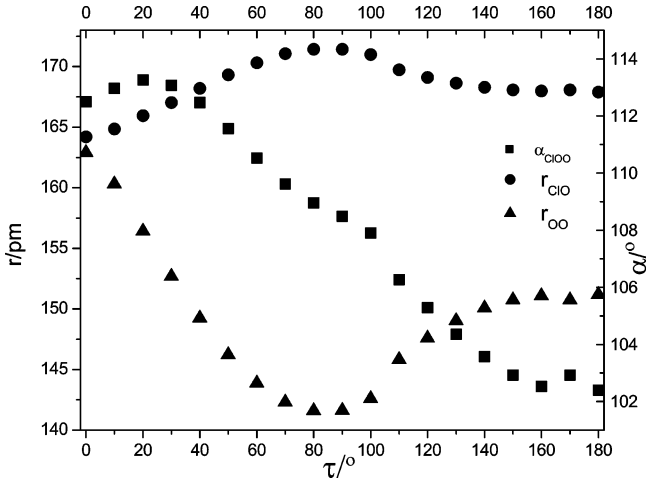

Figure 4. Structure parameters α_{ClOO}, r_{ClO}, and r_{OO} calculated with MP2/aug-cc-pVTZ energy minimization as function of the dihedral angle τ.

TABLE 1: Calculated Equilibrium Geometries of Cl_2O_2 for Various Basis Sets on the MP2 or CCSD(T) Level of Theory[a]

	r_{OO}/pm	r_{ClO}/pm	α_{ClOO}/deg	τ_{ClOOCl}/deg
CCSD(T)/6-31+G*	141.1	176.9	109.6	86.5
CCSD(T)/6-311+G*	136.1	179.4	110.8	85.2
CCSD(T)/aug-cc-pVTZ (I)[c]	140.4	173.4	109.4	83.1
CCSD(T)/aug-cc-pVTZ//MP2/aug-cc-pVTZ[b]	141.6	171.4	108.9	81.8
CCSD(T)/aug-cc-pV(Q+d)Z[75]	140.6	171.5	109.4	82.6
CCSD(T)/TZ2P[59]	141.1	175.3	109.5	84.7
CCSD(T)/ECP-TZDP(f)[62]	141.1	175.3	109.5	84.7
MP2/6-31+G*	142.5	174.3	109.1	85.7
MP2/aug-cc-pVDZ	140.5	176.4	108.9	83.5
MP2/6-311+G*	138.1	175.4	110.4	84.4
MP2/6-311+G(3df)	140.7	170.5	109.1	83.2
MP2/aug-cc-pVTZ (II)[c]	141.6	171.4	108.9	81.8
MP2/aug-cc-pVQZ	141.3	170.4	108.9	81.3
MP2/ECP-TZDP(f)[62]	140.7	171.2	108.9	82.8
MP2/EXTf[59]	141.2	170.5	109.0	82.5
exp.[47]	142.6	170.4	110.1	81.0

[a] For comparison, some results of previous work are also shown. [b] CCSD(T) calculations with the aug-cc-pVTZ basis at the equilibrium geometry optimized on the MP2 level of theory and the aug-cc-pVTZ basis set. [c] See Table 6.

variation is also observed for r_{OO}, which reaches the shortest value for the equilibrium structure and the largest value for the cis structure, whereas r_{ClO} shows only a small variation (for details see the following discussion and Tables 1 and 2). The overall behavior is similar to the corresponding results for the MP2/ECP-TZDP calculations given in ref 62.

Tables 1 and 2 show the calculated equilibrium structures of the low-energy isomer Cl−O−O−Cl as well as the calculated cis and trans transition structures and barrier heights, $V_{el,trans}$ and $V_{el,cis}$ (with $V_{el,trans} = V(\tau = 180°) - V(\tau_{min})$ and $V_{el,cis} = V(\tau = 0°) - V(\tau_{min})$) of the torsional electronic potential energy for various basis sets on the MP2 or CCSD(T) level of theory.

The equilibrium structures (Table 1) calculated with CCSD(T) show in general larger differences between experiment and theory than those for the corresponding MP2 calculations (for the basis sets with moderate size used here).

For the basis sets used in this investigation, the calculated trans saddle point energies for the CCSD(T) calculations are about 1800 cm^{-1}, whereas the MP2 calculations give values in the range of 1300−1500 cm^{-1} (with one exception for MP2/

TABLE 2: Calculated Cis and Trans Transition State Structures (TS) of Cl_2O_2 and Their Corresponding Saddle Point Energies (electronic potential energy: $V_{el,trans} = V_{el}(\tau = 180°) - V_{el}(\tau(Cl_2O_2$, min geo.)) and $V_{el,cis} = V_{el}(\tau = 0°) - V_{el}(\tau(Cl_2O_2$, min. Geo.))) for Various Basis Sets on the MP2 or CCSD(T) Level of Theory

	trans TS: τ_{ClOOCl}/deg = 180				cis TS: τ_{ClOOCl}/deg = 0			
	r_{OO}/pm	r_{ClO}/pm	α_{ClOO}/deg	$V_{el,trans}$/cm^{-1}	r_{OO}/pm	r_{ClO}/pm	α_{ClOO}/deg	$V_{el,cis}$/cm^{-1}
MP2/6-31+G*	153.3	170.3	102.2	1357	160.1	168.2	114.4	3615
MP2/6-311+G*	150.4	169.9	103.0	1713	154.8	168.9	115.9	4107
MP2/ECP-TZDP(f)[a]	152	170	102	1526	152	170	114	3049
MP2/aug-cc-pVTZ	151.2	167.9	102.4	1361	162.9	164.2	112.5	2793
MP2/aug-cc-pVQZ	150.7	167.0	102.6	1329	[c]	[c]	[c]	
CCSD(T)/6-31+G*	153.6	171.2	102.8	1765	161.2	169.3	114.7	3934
CCSD(T)/6-311+G*	150.8	171.0	103.3	2196	156.5	169.9	115.9	4537
CCSD(T)/ECP-TZDP(f)[62]				1890				3538
CCSD(T)/aug-cc-pVTZ	151.0	168.7	103.1	1740	157.9	166.5	114.3	3250
expt[47]				(5660[d])				(3020[d])

[a] Data read out from Figure 1 in ref 62. [b] Trans structure corresponds not to a transition state. TS structures: $r_{OO} = 150.6$ pm, $r_{ClO} = 168.06$ pm, $\alpha = 102.94$, and $\tau = 159.71$ or $\tau = 200.29$. [c] The calculations did not converge. [d] Very roughly estimated from microwave data (see text).[47]

TABLE 3: Calculated Harmonic Wavenumbers ω_i (in cm^{-1}) and Band Strengths G_i (in pm^2) of Cl_2O_2 at the MP2 or CCSD(T) Level of Theory for Various Basis Sets[a]

	CCSD(T)/6-31+G*	CCSD(T)/6-311+G*	CCSD(T)/aug-cc-pVTZ	CCSD(T)/TZ2P[59]	expt[b]
ω_1	766.7	823.5	783.7	767	752[c]/752[d]
G_1				0.201	0.032[d]
ω_2	564.2	522.7	595.1	570	543[c]
G_2				0.387	
ω_3	311.6	293.2	332.2	321	
G_3				0.005	
ω_4	110.6	121.4	116.3	117	127 ± 20[e]
G_4				0.043	
ω_5	623.8	587.6	663.0	629	648[c]/653[d]
G_5				0.636	0.131[d]
ω_6	417.9	402.8	440.5	426	419[c]
G_6				0.175	

	MP2/6-31+G*	MP2/6-311+G*	MP2/aug-cc-pVTZ	MP2/TZDP(f)[59]	MP2/aug-cc-pVQZ
ω_1	748.6	789.9	759.8	775	764.0
G_1	0.158	0.320	0.114		0.107
ω_2	624.0	588.8	640.7	650	648.2
G_2	0.294	0.431	0.155		0.139
ω_3	323.2	325.5	336.0	338	339.0
G_3	0.001	0.008	0.010		0.014
ω_4	109.0	124.6	117.1	117	116.3
G_4	0.069	0.063	0.060		0.059
ω_5	670.4	640.7	699.5	702	708.5
G_5	0.416	0.567	0.285		0.258
ω_6	436.9	438.0	454.6	456	460.3
G_6	0.028	0.179	0.013		0.009

[a] In the following assignments, *s* refers to a stretching and *b* to a bending mode: $\nu_1 = s$(OO), $\nu_2 =$ sym.$-s$(ClO), $\nu_3 =$ asym.$-b$(ClOO), $\nu_4 =$ torsion, $\nu_5 =$ asym.$-s$(ClO), and $\nu_6 =$ asym.$-b$(ClOO). [b] The column "expt." gives experimental results for the fundamentals. [c] Measured in an Ar matrix.[49] [d] Gas-phase measurements.[50] [e] Torsional level energy estimate from intensity distributions in microwave data.[47]

6-311+G* with $V_{trans} = 1713$ cm^{-1}). In the case of the MP2/aug-cc-pVTZ calculation, we found for the optimized $\tau = 180°$ structure an extremely shallow minimum ($\approx$12 cm^{-1} below the correct transition states, see Table 2), which is barely visible in Figure 3. The calculated values for the cis saddle point energies vary considerably as a function of the basis set size even within the same level of theory. However, because the cis saddle point energies are in all cases much higher than the trans saddle point energies, it can be assumed that the cis barrier has only a minor influence on the stereomutation dynamics. As noted before in ref 62, the estimation of the barrier heights from experimental microwave data[47] (with rough estimates of torsional level energies from intensities) is erroneous because the analysis of ref 47 is based on a Fourier series expansion of the potential with three parameters, which is obviously not sufficient to describe the torsional potential shown in Figure 3, which also explains the overestimation of the barrier heights in the experimental analysis[47] as well as the inverted relative magnitude of the cis and trans barriers.

3.2. Harmonic Wavenumbers and Transition Band Strengths. Table 3 presents our results for the harmonic wavenumbers ω_i and the integrated absorption cross sections G_i as well as the corresponding experimental data for fundamental wavenumbers. In Table 4, the calculated harmonic wavenumbers for the corresponding trans and cis structures are given.

By compensation of errors, the harmonic wavenumbers from the coupled cluster calculation with the smallest basis set (6-31+G*) give the best agreement with the experimental data for fundamental wavenumbers. In general, relatively large deviations between experiment and calculations are observed for ω_3, which is the asymmetric ClOO bending vibration. For this mode, even the calculation with the largest basis set (aug-cc-pVTZ) gives results by 10% different from experiment. The overall agreement for the calculations at the MP2 level of theory strongly depends on the vibrational mode considered. The largest differences in the range of about 20% between experiment and theory are observed for ω_2 (sym. s(ClO)). As in the case of the

TABLE 4: Calculated Harmonic Wavenumbers ω_i (in cm^{-1}) at the Trans and Cis Geometry (from Table 2) of Cl_2O_2 at the MP2 or CCSD(T) Level of Theory for Various Basis Sets (negative ω_4 for the reaction coordinate in the case of a transition state)

	MP2/ 6-311+G*	MP2/ aug-cc-pVTZ[a]	CCSD(T)/ 6-311+G*	CCSD(T)/ aug-cc-pVTZ
	trans TS: τ_{ClOOCl}/deg = 180			
ω_1 (A_g)	787.6	808.8	786.4	817.8
ω_2 (A_g)	716.8	727.1	677.4	716.0
ω_3 (A_g)	322.4	328.0	309.8	319.8
ω_4 (A_u)	−25.5	31.2	−44.8	−27.9
ω_5 (B_u)	713.6	746.3	688.2	732.6
ω_6 (B_u)	224.2	227.5	218.6	224.3
	cis TS: τ_{ClOOCl}/deg = 0			
ω_1 (A_1)	652.4	722.0	637.5	701.1
ω_2 (A_1)	478.5	276.9	448.7	473.5
ω_3 (A_1)	211.4	159.0	204.4	213.2
ω_4 (A_2)	−235.2	−134.1	−237.1	−190.3
ω_5 (B_2)	774.0	814.0	755.1	805.8
ω_6 (B_2)	444.7	455.0	424.5	443.1

[a] Not a transition state (see text).

coupled cluster calculations, one has to anticipate that the results are not completely converged as function of the basis set size (at least for basis sets up to quadruple-ζ quality). The calculated integrated absorption cross-sections G_2 and G_5 calculated with the aug-cc-pVTZ or aug-cc-pVQZ basis sets and the MP2 level show a reasonable agreement with the corresponding experimental data, whereas much larger deviations are observed for those of a CCSD(T)/TZ2P calculation.

Although CCSD(T) calculations may be considered to be superior in principle to MP2 calculations, the comparison with experimental results for the fundamental wavenumbers and equilibrium structures does not reflect this expectation for the basis sets employed. Therefore, we decided to use the aug-cc-pVTZ basis set with MP2 in our calculations of the complete reaction path calculation as the best compromise between accuracy and computational cost. This choice also suggests that the calculated tunneling splittings provide upper bounds, because of the comparatively small trans barrier height compared with the coupled cluster results.

3.3. Further Isomers and Transition States. Before we present our calculations of the tunneling splittings, we have to demonstrate that the tunneling process can be well described by our chosen reaction path and alternative competitive tunneling paths are less important. There are at least three further isomers of chlorine dioxide which have comparable relative energies: (i) isomer with branched (C_{2v}) ClO_2 substructure Cl−ClO_2, (ii) isomer with branched (C_{2v}) OCl_2 substructure Cl_2O−O, and (iii) the chain structure ClOClO. The first, Cl−ClO_2, is the lowest energy isomer, about 275 cm^{-1} lower than Cl−O−O−Cl (calculated with MP2/aug-cc-pVTZ), which is consistent with calculations at much higher level.[76] The transition state connecting Cl−O−O−Cl with Cl−ClO_2 is expected to be very high in energy (about the bond dissociation energy of ClO or OO, respectively), and therefore, this isomer has no influence on our conclusions. The second, Cl_2O−O, is calculated to be 2438 cm^{-1} higher in energy than Cl−O−O−Cl. However, calculations at a much higher level yield even a much higher energy difference between these isomers,[76] and therefore, Cl_2O−O also has no importance for the tunneling dynamics of Cl−O−O−Cl. The third isomer, ClOClO, is calculated to be 4230 cm^{-1} higher in energy than Cl−O−O−Cl. For the barrier height connecting these two isomers, we estimate a value of about 6500 cm^{-1} (MP2/aug-cc-pVTZ, transition state structure: $r_{ClO'}$ = 160.3 pm, r_{OO} = 216.2pm, $r_{ClO''}$ = 159.4 pm, $\alpha_{ClO'O''}$ = 88.2°, $\alpha_{O'ClO''}$ = 128.1°, τ_{ClOClO} = 180°) above the minimum of Cl−O−O−Cl. Because of this large barrier height neglecting ClOClO and the corresponding alternative paths for tunneling will not affect our main conclusions. Further high-energy isomers of the ClO dimer such as OClClO or cis-ClOClO (see, e.g., refs 72 and 76) are expected to be even less important for the tunneling dynamics. We will present results of extensive investigations regarding the relative energies of the various isomers and transition states of chlorine dioxide elsewhere.[76]

3.4. Tunneling Splittings. Table 5 summarizes the results for the torsional tunneling splittings in the parity conserving potential

$$\Delta\tilde{\nu}_t = \tilde{\nu}(A^-) - \tilde{\nu}(A^+) \tag{15}$$

of the first 14 pure torsional states (up to the trans barrier height) and the torsional wavenumbers $\tilde{\nu}(A^+)$ with respect to the corresponding zero point level as well as the corresponding band strengths $G_{t,0}$ for transitions from the ground state of Cl_2O_2

TABLE 5: Torsional Tunneling Splittings $\Delta\tilde{\nu}_t = \tilde{\nu}(A^-) - \tilde{\nu}(A^+)$ for Pure Torsional States $|v_t\rangle$ and Band Strengths $G_{t,0} = G(v_t = t(A^-) \leftarrow v = 0(A^+))$ for Transitions from the Rovibrational Ground State $|v = 0(A^+)\rangle$ to $|v_t = t(A^-)\rangle$ of Cl−O−O−Cl

	^{35}Cl−O−O−^{35}Cl			^{35}Cl−O−O−^{37}Cl		^{37}Cl−O−O−^{37}Cl	
v_t[a]	$G_{t,0}$/pm^2	$\Delta\tilde{\nu}_t$/cm^{-1}	$\tilde{\nu}(A^+)$)/cm^{-1}	$\Delta\tilde{\nu}_t$/cm^{-1}	$\tilde{\nu}(A^+)$/cm^{-1}	$\Delta\tilde{\nu}_t$/cm^{-1}	$\tilde{\nu}(A^+)$/cm^{-1}
0	[b]	6.7×10^{-25}	1504.64	5.3×10^{-25}	1500.16	4.1×10^{-25}	1495.7
1	6.8×10^{-3}	5.1×10^{-23}	123.6 (122^{62})[c]	4.1×10^{-23}	122.6 (121^{62})	3.3×10^{-23}	121.4 (119^{62})
2	1.4×10^{-3}	2.0×10^{-21}	245.4 (242^{62})	1.6×10^{-21}	243.3 (240^{62})	1.3×10^{-21}	241.1 (238^{62})
3	9.1×10^{-5}	5.0×10^{-20}	364.9 (361^{62})	4.1×10^{-20}	361.8 (357^{62})	3.3×10^{-20}	358.6 (354^{62})
4	4.6×10^{-6}	9.3×10^{-19}	481.9 (478^{62})	7.5×10^{-19}	477.9 (474^{62})	6.0×10^{-19}	473.8 (469^{62})
5	2.9×10^{-6}	1.4×10^{-17}	596.0	1.1×10^{-17}	591.1	8.7×10^{-18}	586.2
6	1.1×10^{-6}	1.7×10^{-16}	706.8	1.3×10^{-16}	701.2	1.1×10^{-16}	695.5
7	1.4×10^{-7}	2.8×10^{-15}	813.8	2.0×10^{-15}	807.6	1.5×10^{-15}	801.3
8	3.4×10^{-8}	6.1×10^{-13}	916.5	3.5×10^{-13}	909.8	2.0×10^{-13}	903.0
9	6.5×10^{-8}	3.1×10^{-10}	1014.0	1.8×10^{-10}	1007.0	9.9×10^{-11}	999.9
10	9.8×10^{-9}	1.7×10^{-7}	1105.3	9.4×10^{-8}	1098.1	5.2×10^{-8}	1090.8
11	1.3×10^{-10}	1.0×10^{-4}	1188.2	5.5×10^{-5}	1181.3	3.0×10^{-5}	1174.1
12	6.5×10^{-11}	8.2×10^{-2}	1258.5	4.3×10^{-2}	1252.5	2.2×10^{-2}	1246.3
13	8.4×10^{-10}	12.6	1290.5	10.67	1289.2	8.58	1287.6
14	1.3×10^{-10}	19.5	1316.4	19.38	1311.9	19.36	1307.3

[a] v_t is the torsional quantum number in high barrier notation. The corresponding $\tilde{\nu}(A^+)$ are given with respect to the corresponding zero point level, whose approximate wavenumber is given in the line "0". The calculations use the quasi-harmonic quasi-adiabatic channel RPH approximation (MP2/aug-cc-pVTZ). [b] The transition moment for the tunneling transition (the "permanent" electric dipole moment) is 0.70 debye, which can be compared with the electric dipole moment of 0.77 debye for the equilibrium geometry. [c] Torsional level calculations without tunneling and using only the one-dimensional torsional potential (results with CCSD(T)/ECP-TZDP with structures from MP2/ECP-TZDP) are shown in parentheses.[62]

(approximately valid for various chlorine isotopomers, calculations at the MP2 level of theory with the aug-cc-pVTZ basis sets). The calculated tunneling splitting for the vibrational ground state is extremely small, of the order of 10^{-24} cm^{-1}, well below $\Delta_{pv}E$, as we shall see. The calculated band strength $G_{t,0}$ (eq 12) decreases by about an order of magnitude for each additional quantum of torsional excitation with the exception of states comparable in energy with the trans barrier height. The absolute band strength for the torsional fundamental is relatively small (0.067 pm^2). This is about 10% larger than the value calculated within the doubly harmonic approximation (0.06 pm^2 see Table 3), which indicates the presence of some anharmonic contributions.

The isotope effect on the tunneling splitting increases as the energies of the levels reach the energy of the trans barrier height with the largest effect for $\upsilon_t = 12$ (change in $\Delta E_{\pm}$ by a factor of 4 for going from $^{35}Cl_2O_2$ to $^{37}Cl_2O_2$). The isotope effect arises from both the decrease of the torsional energy with increasing mass and the larger reduced tunneling mass. For torsional excitations higher than $\upsilon_t = 12$, the dynamics is dominated by vibrational motion above the trans barrier bounded by the cis barrier potential. Our results for the torsional levels (up to $\upsilon_t = 4$) can be compared with the corresponding results of ref 62 (CCSD(T)/ECP-TZDP) and show a reasonable agreement. However, no tunneling splittings were reported in ref 62. Regarding the accuracy of our tunneling splitting calculations, one should mention that we have demonstrated previously by comparison with experimental results that for the rather similar examples H_2O_2,[35] H_2S_2,[36] and HSOH[37,99] the stereomutation tunneling is well approximated by the present approach. For H_2O_2, a direct validation was provided by comparison of the RPH result with a fully six-dimensional (6D) "exact" discrete variable representation and full dimensional quantum Monte Carlo calculations on the same complete 6D potential hypersurface.[35,94,98] The (approximate) RPH tunneling splittings are generally almost identical to the exact results except in the cases of excited states with local resonances. As described in section 3.1, the torsional barriers calculated with MP2/aug-cc-pVTZ may be somewhat too low and therefore the tunneling splittings for a fully "converged" ab initio calculation are expected to be even smaller than presented in Table 5. However, for the purpose of this work, it is only necessary to estimate an upper limit of the vibrational ground-state tunneling splitting. From the nature of the RPH calculation, the zero point energies given in the line for $\upsilon_t = 0$ are not expected to be accurate, because of the harmonic approximation used for the spectator modes.

3.5. Parity Violating Potentials. The parity violating potential as a function of the torsional angle τ (which is the leading coordinate of the reaction path coordinate) with optimization of all other coordinates is shown in Figure 5. One nicely sees the antisymmetry of E_{pv} about 180° in contrast to the symmetric parity conserving potential. The general form of the parity violating potential E_{pv} for Cl_2O_2 is somewhat different from the corresponding results for H_2O_2, H_2S_2, HSOH, $HOClH^+$, and Cl_2S_2. In all these latter cases, we found a zero crossing with $E_{pv}(\tau) = 0$ at some chiral geometry. For Cl_2O_2, we find no chiral structure along the reaction path for which $E_{pv} = 0$. Only for the achiral, planar structures at 0° and 180° the parity violating potential E_{pv} vanishes, as it must.

The signed electronic parity violating energy difference $\Delta_{pv}E^{el}$ between the two enantiomers at their equilibrium structures is defined as the difference

$$\Delta_{pv}E^{el} = E_{pv}(P) - E_{pv}(M) \qquad (16)$$

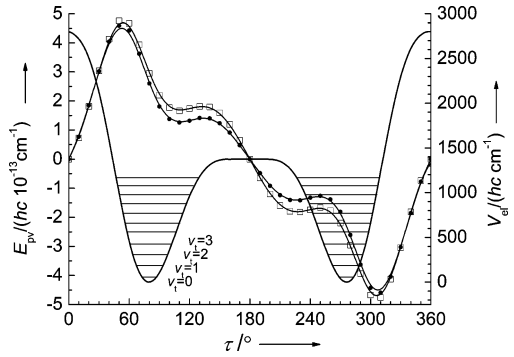

Figure 5. Parity conserving torsional potential $V(\tau)$, shown as a plain full line, as a function of the dihedral angle τ and torsional energy levels for the lower torsional states ($\upsilon_t = 0, 1, 2...$). For these levels, the tunneling splittings are far too small to be visible (see Table 5). For comparison, the corresponding parity violating potentials calculated with RPA/aug-cc-pVTZ (full circles) and RPA/6-311+G(3df) (open squares) are shown. The calculations follow the reaction path in steps of $\Delta\tau = 10°$ with optimization of all structural parameters.

TABLE 6: Parity Violating Energy Differences $\Delta_{pv}E$ Calculated with the MC-LR/RPA Approach at Equilibrium Geometries of $^{35}Cl-O-O-^{35}Cl$ Optimized at Various Levels of Theory and Basis Sets

basis set	$\Delta_{pv}E/10^{-13}(hc)\text{cm}^{-1}$	
	(I)[a]	(II)[b]
6-31G	5.27	5.84
6-31+G	5.80	4.93
6-31G*	4.16	5.53
6-31+G*	4.65	4.87
aug-cc-pVDZ	6.01	5.09
aug-cc-pVTZ	6.02	5.10
6-311+G(3df)	6.21	5.80

[a] For the equilibrium geometry calculated at the CCSD(T)/aug-cc-pVTZ level of theory (see Table 1). [b] For the equilibrium geometry calculated at the MP2/aug-cc-pVTZ level of theory (see Table 1).

Because of the antisymmetry of the parity violating potential with respect to the space inversion, the absolute value of $\Delta_{pv}E^{el}$ is just twice the absolute value of the P or M enantiomer at their equilibrium structure.

$$\Delta_{pv}E^{el} = E_{pv}(P - Cl_2O_2) - E_{pv}(M - Cl_2O_2) \qquad (17)$$

$$|\Delta_{pv}E^{el}| = 2|E_{pv}(P - Cl_2O_2)| \approx |\Delta_R H_0^{\ominus}/N_A| \approx (hc)6 \times 10^{-13}\ \text{cm}^{-1} \qquad (18)$$

$\Delta_R H_0^{\ominus}$ corresponds to an in principle measurable ground-state energy difference or reaction enthalpy at 0 K ($\approx 7 \times 10^{-12}$ J mol^{-1}). Strictly speaking, one would have to carry out vibrational averaging in order to obtain an accurate prediction for this measurable energy,[100] but $\Delta_{pv}E^{el}$ is an acceptable approximation in many cases. Table 6 summarizes $\Delta_{pv}E^{el}$ for two structures of Cl_2O_2 (calculated as equilibrium geometries with either CCSD(T)/aug-cc-pVTZ or MP2/aug-cc-pVTZ) for various basis sets. There is only a modest basis set dependence. The values show that (M)-Cl_2O_2 is stabilized compared to (P)-Cl_2O_2 by about 6×10^{-13} cm^{-1}.

An expectation value of $\langle\Delta_{pv}E\rangle/hc = 5.7 \times 10^{-13}$ cm^{-1}was also calculated employing the parity violating potential calculated with RPA/6-311+G(3df) and averaging over the lowest (ground state) wave function from the RPH, which is almost identical with the value calculated at the equilibrium geometry $\Delta_{pv}E/hc = 5.8 \times 10^{-13}$ cm^{-1} for this case. Therefore, the effect of vibrational averaging is small and is expected to be even

smaller for the other vibrational degrees of freedom. The corrections are of similar order of magnitude as the scatter due to the basis set dependence shown in Table 6. For ^{35}Cl−O−O−^{35}Cl, ^{35}Cl−O−O−Cl^{37}, and ^{37}Cl−O−O−^{37}Cl, the isotope effect on the value of $\Delta_{pv}E^{el}$ calculated at the equilibrium (r_e) structure is very small. Somewhat larger isotope effects might arise from vibrational averaging of the parity violating potential,[43] because of the slightly different r_0 structures of the isotopomers in combination with the geometry dependence of the parity violating potential.

We conclude that $\Delta_{pv}E$ is about 12 orders of magnitude larger than the vibrational ground-state torsional tunneling splittings $\Delta E_{\pm}$ of the hypothetical parity conserving electronic potential. Thus, tunneling is suppressed, and all low-lying eigenstates, for which $\Delta_{pv}E \gg \Delta E_{\pm}$ is valid (here up to $v_t = 7$, see Table 1), have a well-defined chirality (*P* or *M*) corresponding to the case de lege symmetry breaking[2] where parity violation dominates the dynamics of stereomutation in Cl−O−O−Cl.

"Tunneling switching" occurs at a modest torsional excitation of about 1000 cm^{-1} or more. At higher levels, tunneling splittings dominate over parity violation and thus each rotation−vibration−tunneling level has a well-defined parity. Excitation with a narrow band pump IR laser in a frequency range above 1100 cm^{-1} (almost accessible to the CO_2 laser) thus would allow one to achieve a parity selection following the scheme of Figure 1, and with a subsequent dump IR laser pulse following,[23] one would generate a superposition state of well-defined parity (because of the dominant electric dipole selection rule) but in an energy range where the dynamics is in fact dominated by parity violation. Thus, the prepared superposition state of a well-defined parity, say around 500 cm^{-1}, would evolve in time due to parity violation, into a state of opposite parity with a half period

$$\tau_{pv}/2 = h/(2\Delta_{pv}E) \simeq 28s \qquad (19)$$

As the collision and field free conditions (including spontaneous emission) needed for such an experiment cannot be maintained for such a long period, one would aim at the detection of an initially forbidden signal, again by high-resolution IR spectroscopy combined with a sensitive detection scheme, such as IR-UV-REMPI ionization detection as used in isotope selective overtone spectroscopy.[101,102] The probability of a "forbidden" line signal will change with time according to ($\tau \equiv \tau_{pv}$)

$$p_f(t) = \sin^2(\pi t/\tau) \qquad (20)$$

which can be approximated by a quadratically increasing signal $p_f(t) \approx (\pi t/\tau)^2$ for small times. Taking 10 ms as a realistic upper time range for such experiments, one would need a detection sensitivity and discrimination against the background signals of better than about 10^{-7}, which is not unrealistic. The considerations are very similar to those applicable with UV−vis spectroscopy involving excited intermediate electronic states with rovibrational levels of well-defined parity.[23,33] In considering the advantages and drawbacks of experiments in the two spectral ranges, one notes the much higher resolution and thus selective state preparation which can be achieved in the IR, compared to visible laser state preparation and detection. Also, the natural line widths are much smaller and the lifetimes for spontaneous emission are much longer in the IR. A drawback with IR schemes is the potentially higher background signal from thermally excited molecules that might not be completely cooled in the supersonic beam expansions which are probably to be used in all such experiments.

It should also be clear that one may not be able or even not wish to pass via direct excitation of high torsional overtone levels. For a transition from the vibrational ground state to a state with $v_t = 11$, we have estimated a band strength of only $G(v_t = 11(A^-) \leftarrow v_0(A^+)) = 1.3 \times 10^{-10}$ pm^2 (Table 5).

One might therefore choose sequential excitation schemes, because for all pure torsional states with $v_t \leq 7$ the condition $\Delta_{pv}E > \Delta E_{\pm}$ is fulfilled. If within such a scheme the excitation of the state with $v_t = 7$ is feasible, then a transition to a state should be possible for which $\Delta_{pv}E < \Delta E_{\pm}$ is valid, for example, $v_t = 11$. We estimate, for example, $G(v_t = 11(A^-) \leftarrow v_t = 7(A^+)) = 8.1 \times 10^{-3}$ pm^2, which is sufficiently large for efficient excitation. Furthermore, the corresponding state with positive parity with $v_t = 11(A^+)$ is reasonably well separated (by 1×10^{-4} cm^{-1}), if the experiment is carried out under Doppler-free conditions. Another alternative is to excite a low overtone of a higher frequency mode, searching for an "accidental" resonance coupling of such a level with a high overtone of the torsion even above the barrier. This could lead as well to the desired parity selection. Figure 6 shows an energy level scheme of Cl_2O_2 including rough estimates for all combination and overtone states. It is clear that above 1000 cm^{-1} the density of levels is sufficiently high to allow for ample opportunities for such resonances. While these would have to be identified in a first step, the high density of levels with increasing energy has also the risk of generating undesired background absorption signals. Of course, our exploratory calculations on Cl_2O_2 are meant to identify a possible, but not necessarily the best, candidate for realizing such a scheme, illustrated here with quantitative numerical predictions for our example.

4. Conclusions and Outlook

We have shown in previous work that accurate predictions for the tunneling stereomutation dynamics in X−Y−Z−X′ molecules analogous to hydrogen peroxide H−O−O−H are possible by combining the quasi-adiabatic channel reaction path Hamiltonian approach with suitable ab initio calculations (Table 7).[34−39,41] Here, we have made use of this knowledge in order to predict the torsional tunneling dynamics in Cl−O−O−Cl from the ground state to high torsional excitation. A comparison with calculations of the parity violating energy difference $\Delta_{pv}E$ between the two enantiomers of the nonplanar, chiral Cl−O−O−Cl molecule shows that, indeed, in the ground state, the tunneling splitting $\Delta E_{\pm}$ is almost 12 orders of magnitude smaller than $\Delta_{pv}E$. This finding implies that at low energies the quantum dynamics of Cl−O−O−Cl is dominated by the seemingly tiny effects arising from the parity violating electroweak interaction and that the parity violating energy difference between enantiomers corresponds to a measurable quantity, in principle.[2,23]

We have furthermore shown that at moderate torsional excitations in the IR range around 1200 cm^{-1} (with $v_t \simeq 11-13$) the torsional tunneling splittings $\Delta E_{\pm}$ become much larger than $\Delta_{pv}E$. Thus, the experimental scheme of refs 2 and 23 (see also ref 4 for further variants), which is based on spectroscopic parity selection and observation of time-dependent parity evolution or combination differences, could be realized in principle in the Cl_2O_2 molecule using only excitations in the IR by "tunneling switching" (see Figure 1). While this molecule may not necessarily be the best choice for such an investigation, it provides us with a proof of principle prediction for a realistic situation. As is shown by Table 7, a suitable change of composition of the X−Y−Z−X′ molecules allows one to tune $\Delta_{pv}E$ (by the approximate Z^5 scaling, see refs 10−14) and $\Delta E_{\pm}$ (by the scaling of barriers and effective tunneling masses). In

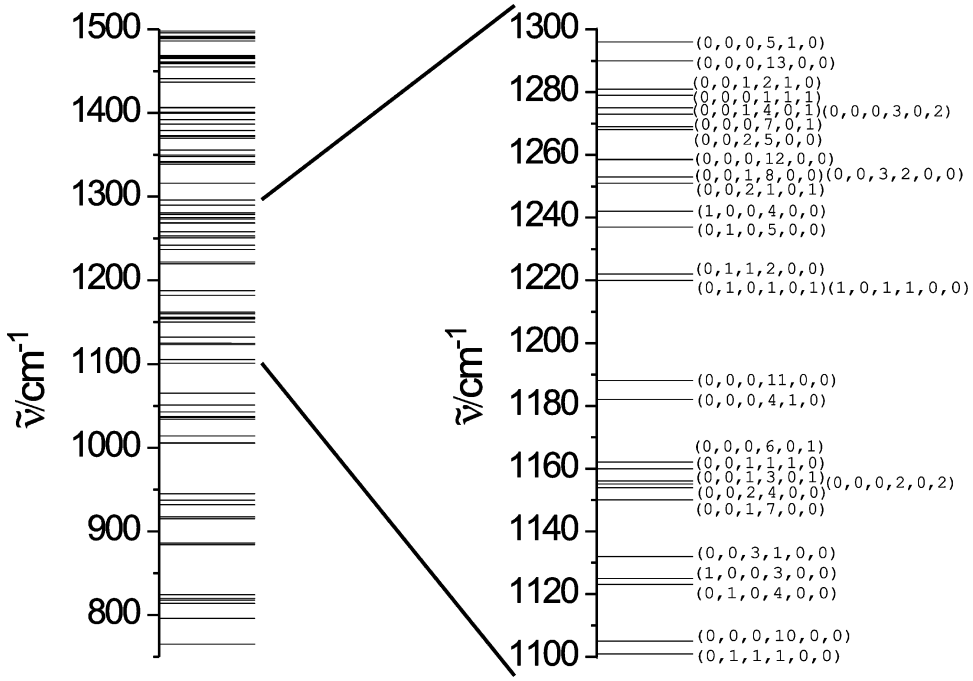

Figure 6. Level scheme of all possible vibrational overtones and combination bands in the energy range between 750 and 1500 cm^{-1} (90 bands in total). For the energy region between 1100 and 1300 cm^{-1} (which includes the torsional states with $v_t = 10$ up to $v_t = 13$, for which $\Delta_{pv}E \ll \Delta E_{\pm}$), the states are explicitly assigned with the convention: (v_1, v_2, v_3, v_4, v_5, v_6).

TABLE 7: Survey of Theoretically Calculated $|\Delta_{pv}E^{el}|$[a] and $\Delta E_{\pm}$ for Various X−Y−Z−X′ Molecules

molecule	$\lvert\Delta_{pv}E^{el}\rvert/hc$·cm^{-1}	$\Delta E_{\pm}/hc$·cm^{-1}	ref
H_2O_2	4×10^{-14}	11	10−13, 35, 104
D_2O_2	4×10^{-14}	2	13, 35
T_2O_2	4×10^{-14}	0.5	37
HSOH	4×10^{-13}	2×10^{-3}	37
DSOD	4×10^{-13}	1×10^{-5}	37
TSOT	4×10^{-13}	3×10^{-7}	37
$HClOH^+$	8×10^{-13}	2×10^{-2}	40
$DClOD^+$	[b]	2×10^{-4}	40
$TClOT^+$	[b]	7×10^{-6}	40
H_2S_2	1×10^{-12}	2×10^{-6}	36
D_2S_2	1×10^{-12}	5×10^{-10}	36
T_2S_2	1×10^{-12}	1×10^{-12}	36
Cl_2O_2	6×10^{-13}	7×10^{-25}	this work
Cl_2S_2	1×10^{-12}	$\approx 10^{-76}$ [c]	38
H_2Se_2	2×10^{-10}[d]	1×10^{-6}	16, 39
D_2Se_2	[e]	3×10^{-10}	39
T_2Se_2	[e]	4×10^{-13}	39
H_2Te_2	3×10^{-9} [f]	3×10^{-8}	16, 40
D_2Te_2	[g]	1×10^{-12}	40
T_2Te_2	[g]	3×10^{-16}	40

[a] Values for $\Delta_{pv}E^{el}$ are calculated at the equilibrium structures of the corresponding compounds (without vibrational corrections). [b] Expected to be similar to the value for $HClOH^+$. [c] Extrapolated value. [d] Calculated for the *P*-structure ($r_{SeSe} = 248$ pm, $r_{HSe} = 145$ pm, $\alpha_{HSeSe} = 92°$, and $\tau_{HSeSeH} = 90°$) and the corresponding *M*-structure.[16] An earlier, very approximate result by Wiesenfeld[8] may be quoted as well, giving $\Delta_{pv}E = 6 \times 10^{-10}$ cm^{-1} for the following structure: $r_{SeSe} = 232.5$ pm, $r_{HSe} = 146$ pm, $\alpha_{HSeSe} = 90°$, and $\tau_{HSeSeH} = 90°$. [e] Expected to be very similar to the corresponding value for H_2Se_2. [f] Calculated for the *P*-structure ($r_{TeTe} = 284$ pm, $r_{HTe} = 164$ pm, $\alpha_{HTeTe} = 92°$ and $\tau_{HTeTeH} = 90°$) and the corresponding *M*-structure.[16] An earlier, very approximate result by Wiesenfeld[8] may be quoted as well, giving $\Delta_{pv}E = 8 \times 10^{-10}$ cm^{-1} for the following structure: $r_{TeTe} = 271.2$ pm, $r_{HTe} = 165.8$ pm, $\alpha_{HTeTe} = 90°$, and $\tau_{HTeTeH} = 90°$. [g] Expected to be similar to the value for H_2Te_2.

considering this scaling, as apparent also in Table 7, one might be tempted to consider with preference molecules with heavy central atoms Y−Z (for a large $\Delta_{pv}E$) and light to moderately heavy substituents (X, X′), to allow for adequate tunneling switching at moderate excitations in the IR. This would, in any case, provide us with an interesting alternative to the route via excited electronic states, for which 1,3-difluoroallene was identified as a realistic candidate.[33]

The use of molecules with heavy nuclei may require further consideration. While the observation of molecular parity violation would be of some interest per se, but not fundamentally new, as it is certainly predicted by the now well-established and experimentally confirmed electroweak theory, a more important long-term goal of such molecular spectroscopic experiments would be to gain insights into the parameters of the standard model beyond knowledge available from high-energy physics experiments[1] (see refs 4 and 12 for a discussion). For instance, one might obtain a variation of the value for the Weinberg parameter $\sin^2 \Theta_W$ at low energy (or low four momentum transfer Q) as it has been attempted already in atomic and electron scattering experiments.[105−107] This requires in both the atomic and the still hypothetical future molecular case a comparison of accurate experimental and theoretical results for parity violation. It turns out that the theoretical uncertainties for the heavy atom (Cs, etc.) experiments are actually an important source of uncertainty and it is very unlikely that molecular calculations involving such heavy atoms will be more accurate than the corresponding atomic calculations. The advantage of the molecular experiment would be, however, that it should be feasible involving only light elements of the first rows of the periodic table, for which much more accurate calculations should be possible. Thus, also in this sense, Cl_2O_2 and similar molecules may be good prototype systems for a molecular route toward electroweak theory and the standard model.

While the results on stereomutation and parity violation in Cl_2O_2 are the most important aspects of the present work, our predictions of the spectroscopic properties of Cl_2O_2 are also of interest for a reassessment of the spectroscopy of this molecule, so important as trace gas for the chemistry of the earth's atmosphere.[55,56] Our results should help to plan new and more

accurate spectroscopic experiments and also more accurate theoretical calculations of the spectroscopic and thermochemical properties, which will be reported elsewhere.[76]

Acknowledgment. Our work is supported financially by the ETH Zürich and the Schweizerischer Nationalfonds (including C4 and CSCS). We enjoyed fruitful discussions with Sieghard Albert, Robert Berger, Sofia Deloudi, Michael Gottselig, Hans Hollenstein, Ľuboš Horný, David Luckhaus, Carine Manca, H. F. Schaefer III, Achim Sieben, and Jürgen Stohner.

References and Notes

(1) Hoddeson, L.; Brown, L.; Riordan, M.; Dresden, M. *The Rise of the Standard Model*; Cambridge University Press: Cambridge, U.K., 1997.
(2) Quack, M. *Angew. Chem., Int. Ed. Engl.* **1989**, *28*, 571.
(3) Frank, P.; Bonner, W. A.; Zare, R. N. In *Chemistry for the 21st Century*; Keinan, E., Schechter, I., Eds.; Wiley-VCH: Weinheim, Germany, 2001; pp 175−208.
(4) Quack, M. *Angew. Chem., Intl. Ed.* **2002**, *41*, 4618.
(5) Hegstrom, R. A.; Rein, D. W.; Sandars, P. G. H. *J. Chem. Phys.* **1980**, *73*, 2329.
(6) Mason, S.; Tranter, G. *Mol. Phys.* **1984**, *53*, 1091.
(7) MacDermott, A. J.; et al. *Planet. Space Sci.* **1996**, *44*, 1441.
(8) Wiesenfeld, L. *Mol. Phys.* **1988**, *64*, 739.
(9) Kiyonaga, H.; Morihashi, K.; Kikuchi, O. *J. Chem. Phys.* **1998**, *108*, 2041.
(10) Bakasov, A.; Ha, T. K.; Quack, M. Ab initio calculation of molecular energies including parity violating interactions. In *Proceedings of the 4th Trieste Conference 1995, Chemical Evolution: Physics of the Origin and Evolution of Life*; Chela-Flores, J., Rolin, F., Eds.; Kluwer Academic Publishers: Dordrecht, The Netherlands, 1996; pp 287−296.
(11) Bakasov, A.; Ha, T. K.; Quack, M. *J. Chem. Phys.* **1998**, *109*, 7263. Erratum: *J. Chem. Phys.* **1999**, *110*, 6081.
(12) Bakasov, A.; Quack, M. *Chem. Phys. Lett.* **1999**, *303*, 547.
(13) Berger, R.; Quack, M. *J. Chem. Phys.* **2000**, *112*, 3148.
(14) Bakasov, A.; Berger, R.; Ha, T. K.; Quack, M. *Int. J. Quantum Chem.* **2004**, *98*, 393.
(15) Lazzeretti, P.; Zanasi, R. *Chem. Phys. Lett.* **1997**, *279*, 349.
(16) Laerdahl, J. K.; Schwerdtfeger, P. *Phys. Rev. A* **1999**, *60*, 4439.
(17) Hennum, A. C.; Helgaker, T.; Klopper, W. *Chem. Phys. Lett.* **2002**, *354*, 274.
(18) Letokhov, V. S. *Phys. Lett. A* **1975**, *53*, 275.
(19) Kompanets, O. N.; Kukudzhanov, A. R.; Letokhov, V. S.; Gervits, L. L. *Opt. Commun.* **1976**, *19*, 414.
(20) Arimondo, E.; Glorieux, P.; Oka, T. *Opt. Commun.* **1977**, *23*, 369.
(21) Harris, R. A.; Stodolski, L. *Phys. Lett. B* **1978**, *78*, 313.
(22) Barra, A. L.; Robert, J. B.; Wiesenfeld, L. *Biosystems* **1987**, *20*, 57.
(23) Quack, M. *Chem. Phys. Lett.* **1986**, *132*, 147.
(24) Pepper, M. J. M.; Shavitt, I.; Schleyer, P. v. R.; Glukhovtsev, M. N.; Janoschek, R.; Quack, M. *J. Comput. Chem.* **1995**, *16*, 207.
(25) Bauder, A.; Beil, A.; Luckhaus, D.; Müller, F.; Quack, M. *J. Chem. Phys.* **1997**, *106*, 7558.
(26) Daussy, C.; Marrel, T.; Amy-Klein, A.; Nguyen, C. T.; Borde, C. J.; Chardonnet, C. *Phys. Rev. Lett.* **1999**, *83*, 1554.
(27) Lahamer, A. S.; Mahurin, S. M.; Compton, R. N.; House, D.; Laerdahl, J. K.; Lein, M.; Schwerdtfeger, P. *Phys. Rev. Lett.* **2000**, *85*, 4470.
(28) Quack, M.; Stohner, J. *Phys. Rev. Lett.* **2000**, *84*, 3807.
(29) Quack, M.; Stohner, J. *Z. Physik. Chem.* **2000**, *214*, 675.
(30) Quack, M.; Stohner, J. *Chirality* **2001**, *13*, 745.
(31) Stohner, J.; Quack, M. *Chimia* **2005**, *59*, 530.
(32) Laerdahl, J. K.; Schwerdtfeger, P.; Quiney, H. M. *Phys. Rev. Lett.* **2000**, *84*, 3811.
(33) Gottselig, M.; Quack, M. *J. Chem. Phys.* **2005**, *123*, 084305.
(34) Fehrensen, B.; Luckhaus, D.; Quack, M. *Z. Phys. Chem.* **1999**, *209*, 1.
(35) Fehrensen, B.; Luckhaus, D.; Quack, M. *Chem. Phys. Lett.* **1999**, *300*, 312.
(36) Gottselig, M.; Luckhaus, D.; Quack, M.; Stohner, J.; Willeke, M. *Helv. Chim. Acta* **2001**, *84*, 1846.
(37) Quack, M.; Willeke, M. *Helv. Chim. Acta* **2003**, *86*, 1641.
(38) Berger, R.; Gottselig, M.; Quack, M.; Willeke, M. *Angew. Chem., Intl. Ed.* **2001**, *40*, 4195.
(39) Gottselig, M.; Quack, M.; Willeke, M. *Isr. J. Chem.* **2003**, *43*, 353.
(40) Gottselig, M.; Quack, M.; Stohner, J.; Willeke, M. *Int. J. Mass Spectrom.* **2004**, *233*, 373.
(41) Fehrensen, B.; Luckhaus, D.; Quack, M.; Willeke, M.; Rizzo, T. *J. Chem. Phys.* **2003**, *119*, 5534.
(42) Berger, R.; Quack, M.; Sieben, A.; Willeke, M. *Helv. Chim. Acta* **2003**, *86*, 4048.
(43) Berger, R.; Laubender, G.; Quack, M.; Sieben, A.; Stohner, J.; Willeke, M. *Angew. Chem., Int. Ed.* **2005**, *44*, 3623.
(44) Burkholder, J. B.; Orlando, J. J.; Howard, C. J. *J. Phys. Chem.* **1990**, *94*, 687.
(45) Molina, L. T.; Molina, M. J. *J. Phys. Chem.* **1987**, *91*, 433.
(46) DeMore, W. B.; Tschuikov-Roux, E. *J. Phys. Chem.* **1990**, *94*, 5856.
(47) Birk, M.; Friedl, R. R.; Cohen, E. A.; Pickett, H. M.; Sander, S. P. *J. Chem. Phys.* **1989**, *91*, 6588.
(48) Cheng, B.-M.; Lee, Y.-P. *J. Chem. Phys.* **1989**, *90*, 5930.
(49) Jacobs, J.; Kronberg, M.; Müller, H. S. P.; Willner, H. *J. Am. Chem. Soc.* **1994**, *116*, 1106.
(50) Brust, A. S.; Zabel, F.; Becker, K. H. *Geophys. Res. Lett.* **1997**, *24*, 1395.
(51) Bloss, W. J.; Nickolaisen, S. L.; Salawitch, R. J.; Friedl, R. R.; Sander, S. P. *J. Phys. Chem. A* **2001**, *105*, 11226.
(52) Horvath, A.; Nagypal, I.; Peintler, G.; Epstein, I. R.; Kustin, K. *J. Phys. Chem. A* **2003**, *107*, 6966.
(53) Stimpfle, R. M.; Wilmouth, D. M.; Salawitch, R. J.; Anderson, J. G. *J. Geophys. Res.* **2004**, *109*, D03301.
(54) Schwell, M.; Jochims, H.-W.; Wassermann, B.; Rockland, U.; Flesch, R.; Rühl, E. *J. Phys. Chem.* **1996**, *100*, 10070.
(55) Molina, M. J. *Angew. Chem., Int. Ed. Engl.* **1996**, *35*, 1778.
(56) Rowland, F. S. *Angew. Chem., Int. Ed. Engl.* **1996**, *35*, 1786.
(57) McGrath, M. P.; Clemitshaw, K. C.; Rowland, F. S.; Hehre, W. J. *J. Phys. Chem.* **1990**, *94*, 6126.
(58) Jensen, F.; Oddershede, J. *J. Phys. Chem.* **1990**, *94*, 2235.
(59) Lee, T. J.; Rohlfing, C. M.; Rice, J. E. *J. Chem. Phys.* **1992**, *97*, 6593.
(60) Francisco, J. S.; Sander, S. P. *J. Chem. Phys.* **1995**, *192*, 9615.
(61) Luke, B. T. *J. Mol. Struct. (THEOCHEM)* **1995**, *332*, 283.
(62) Gómez, P. C.; Pacios, L. F. *J. Phys. Chem.* **1996**, *100*, 8731.
(63) Gleghorn, J. T. *Chem. Phys. Lett.* **1997**, *271*, 296.
(64) Han, Y.-K.; Kim, K. H.; Lee, Y. S.; Baeck, K. K. *J. Mol. Struct. (THEOCHEM)* **1998**, *431*, 185.
(65) Christen, D.; Mack, H.-G.; Müller, H. S. P. *J. Mol. Struct.* **1999**, *509*, 137.
(66) Charkin, O. P.; Klimenko, N. M.; McKee, M. L. *Russ. J. Inorg. Chem.* **2000**, *45*, 1369.
(67) Escribano, R.; Mosteo, R. G.; Gómez, P. C. *Can. J. Phys.* **2001**, *79*, 597.
(68) Papayannis, D. K.; Melissas, V. S.; Kosmas, A. M. *Chem. Phys. Lett.* **2001**, *349*, 299.
(69) Jalbout, A. F. *J. Mol. Struct. (THEOCHEM)* **2002**, *592*, 123.
(70) Jalbout, A. F. *J. Mol. Struct. (THEOCHEM)* **2002**, *594*, 1.
(71) Tomasello, P.; Ehara, M.; Nakatsuji, H. *J. Chem. Phys.* **2002**, *116*, 2425.
(72) Li, Q.; Lü, S.; Xie, Y.; Schleyer, P. v. R.; Schaefer, H. F., III. *Int. J. Quantum Chem.* **2003**, *95*, 731.
(73) Zhu, R. S.; Lin, M. C. *J. Chem. Phys.* **2003**, *118*, 4094.
(74) Zhu, R. S.; Lin, M. C. *J. Phys. Chem. A* **2003**, *107*, 3836.
(75) Peterson, K. A.; Francisco, J. S. *J. Chem. Phys.* **2004**, *121*, 2611.
(76) Horný, Ľ; Quack, M.; Schaefer, H. F, III; Willeke, M.; *Proceedings of the 28th International Symposium on Free Radicals, Leysin*; Maier, J. P., Ed.; 2005; p 110 and in preparation.
(77) Frisch, M. J.; Trucks, G. W.; Schlegel, H. B.; Scuseria, G. E.; Robb, M. A.; Cheeseman, J. R.; Montgomery, J. A., Jr.; Vreven, T.; Kudin, K. N.; Burant, J. C.; Millam, J. M.; Iyengar, S. S.; Tomasi, J.; Barone, V.; Mennucci, B.; Cossi, M.; Scalmani, G.; Rega, N.; Petersson, G. A.; Nakatsuji, H.; Hada, M.; Ehara, M.; Toyota, K.; Fukuda, R.; Hasegawa, J.; Ishida, M.; Nakajima, T.; Honda, Y.; Kitao, O.; Nakai, H.; Klene, M.; Li, X.; Knox, J. E.; Hratchian, H. P.; Cross, J. B.; Adamo, C.; Jaramillo, J.; Gomperts, R.; Stratmann, R. E.; Yazyev, O.; Austin, A. J.; Cammi, R.; Pomelli, C.; Ochterski, J. W.; Ayala, P. Y.; Morokuma, K.; Voth, G. A.; Salvador, P.; Dannenberg, J. J.; Zakrzewski, V. G.; Dapprich, S.; Daniels, A. D.; Strain, M. C.; Farkas, O.; Malick, D. K.; Rabuck, A. D.; Raghavachari, K.; Foresman, J. B.; Ortiz, J. V.; Cui, Q.; Baboul, A. G.; Clifford, S.; Cioslowski, J.; Stefanov, B. B.; Liu, G.; Liashenko, A.; Piskorz, P.; Komaromi, I.; Martin, R. L.; Fox, D. J.; Keith, T.; Al-Laham, M. A.; Peng, C. Y.; Nanayakkara, A.; Challacombe, M.; Gill, P. M. W. *Gaussian 03*, revision C.02; Gaussian, Inc.: Wallingford, CT, 2003.
(78) McLean, A. D.; Chandler, G. S. *J. Chem. Phys.* **1980**, *72*, 5639.
(79) Pople, J. A. *J. Chem. Phys.* **1980**, *72*, 650.
(80) Curtiss, L. A.; McGrath, M. P.; Blandeau, J.-P.; Davis, N. E.; Binning, R. C.; Radom, J. L. *J. Chem. Phys.* **1995**, *103*, 6104.
(81) Woon, D. E.; Dunning, T. *J. Chem. Phys.* **1993**, *98*, 1358.
(82) Quack, M. *Annu. Rev. Phys. Chem.* **1990**, *41*, 839.
(83) Quack, M.; Stohner, J. *J. Chem. Phys.* **2003**, *119*, 11228.
(84) Cvitaš, T.; Frey, J.; Holmström, B.; Kuchitsu, K.; Marquardt, R.; Mills, I.; Pavese, F.; Quack, M.; Stohner, J.; Strauss, H. L.; Takami, M.; Thor, A. J. *Quantities, Units and Symbols in Physical Chemistry*; IUPAC, 2006, in preparation.

(85) Helgaker, T.; Jensen, H. J. Aa.; Joergensen, P.; Olsen, J.; Ruud, K.; Aagren, H.; Auer, A. A.; Bak, K. L.; Bakken, V.; Christiansen, O.; Coriani, S.; Dahle, P.; Dalskov, E. K.; Enevoldsen, T.; Fernandez, B.; Haettig, C. Hald, K.; Halkier, A.; Heiberg, H.; Hettema, H.; Jonsson, D.; Kirpekar, S.; Kobayashi, R.; Koch, H.; Mikkelsen, K. V.; Norman, P.; Packer, M. J.; Pedersen, T. B.; Ruden, T. A.; Sanchez, A.; Saue, T.; Sauer, S. P. A.; Schimmelpfennig, B.; Sylvester-Hvid, K. O.; Taylor, P. R.; Vahtras, O. *Dalton release 1.0, an electronic structure program*, 1997.

(86) Berger, R.; Quack, M.; Stohner, J. *Angew. Chem., Intl. Ed.* **2001**, *40*, 1667.

(87) Berger, R.; Quack, M. *ChemPhysChem* **2000**, *1*, 57.

(88) Miller, W. H.; Handy, N. C.; Adams, J. E. *J. Chem. Phys.* **1980**, *72*, 99.

(89) Quack, M.; Troe, J. Statistical Adiabatic Channel Model. In *Encyclopedia of Computational Chemistry*; Schleyer, P. v. R., Allinger, N., Clark, T., Gasteiger, J., Kollman, P. A., Schaefer, H. F., III, Schreiner, P. R., Eds.; John Wiley and Sons: New York, 1998; Vol. 4, pp 2708−2726.

(90) Quack, M.; Troe, J. *Ber. Bunsen-Ges. Phys. Chem.* **1974**, *78*, 240.

(91) Quack, M.; Troe, J. Unimolecular Reactions and Energy Transfer of Highly Excited Molecules. In *Gas Kinetics and Energy Transfer*; Ashmore, P. G., Donovan, R. J., Eds.; The Chemical Society: London, 1977; Vol 2, pp 175−238.

(92) Quack, M.; Troe, J. *Theor. Chem.: Adv. Perspect. B* **1981**, *6*, 199.

(93) Meyer, R. *J. Chem. Phys.* **1970**, *52*, 2053.

(94) Luckhaus, D. *J. Chem. Phys.* **2000**, *113*, 1329.

(95) Luckhaus, D.; Quack, M. *Chem. Phys. Lett.* **1992**, *190*, 581.

(96) Bacic, Z.; Light, J. C. *Annu. Rev. Phys. Chem.* **1989**, *40*, 469.

(97) Light, J. C.; Carrington, T. *Adv. Chem. Phys.* **2000**, *114*, 263.

(98) Kuhn, B.; Rizzo, T. R.; Luckhaus, D.; Quack, M.; Suhm, M. *J. Chem. Phys.* **1999**, *111*, 2565.

(99) Yamada, K. M. T.; Winnewisser, G.; Jensen, P. *J. Mol. Spectrosc.* **2004**, *695*−*696*, 323.

(100) Quack, M.; Stohner, J. *J. Chem. Phys.* **2003**, *119*, 11228.

(101) Hippler, M.; Pfab, R.; Quack, M. *J. Phys. Chem.* **2003**, *107*, 10743.

(102) Hippler, M.; Quack, M. *J. Chem. Phys.* **1996**, *104*, 7426.

(103) Garg, A. *Am. J. Phys.* **2000**, *68*, 430.

(104) Olson, W. B.; Hunt, R. H.; Young, B. W.; Maki, A. G.; Brault, J. W. J. *J. Mol. Spectrosc.* **1988**, *128*, 12.

(105) Bennet, S. C.; Wieman, C. E. *Phys. Rev. Lett.* **1999**, *82*, 2484.

(106) Czarnicky, A.; Marciano, W. J. *Int. J. Mod. Phys. A* **2000**, *15*, 2365.

(107) Anthony, P. L.; et al. *Phys. Rev. Lett.* **2005**, *95*, 081601−1.

(108) Schwarzschild, B. *Phys. Today* **2005**, *58*, 23.